OPEN ACCESS
Freely Available Online

JOURNAL OF ADVANCES IN NANOTECHNOLOGY
ISSN NO: 2689-2855

Review

DOI: 10.14302/issn.2689-2855.jan-19-3048

The Study of Coexistance of Superconductivity and Spin Glass in Fe Pnictide($Fe1+YSeXTe1-X$)

Anteneh Yesigat[1,*], Psingh[2]

[1]Addis Ababa University, Addis Ababa, Ethiopia

[2]Kotebe Metropolitan University, Addis Ababa, Ethiopia

Abstract

Superconductivity and magnetism were previously thought as incompatible until the discovery of some rare earth ternary compounds that shows the coexistence of superconductivity and magnetism. In some of the recently discovered iron based layered superconductors superconductivity and diamagnetic order system are coexist. That occurs in only 11 and 122 family. The present works we examine the possibility of coexistence of superconductivity and disorder of magnetic spin is called spin glass when freeze the system that can show the superconductivity and spin glass coexist. In this present work we can examine the possibility of coexistence of superconductivity and spin glass in detailed 11 family of $Fe1+ySexTe1-x$ compound. We show that spin glass like behavior is present in FST for x = 0.1 - 0.15 we present evidence form magnetization measurement and characterized the short-range order with neutron scattering. One of our main results is that the short-range order is structural as well as magnetic order. The factor of magnetic order exchange in long range depend on temperature, pressure, number of doping and other external factor discussed it. We found mathematical expression for superconductor transition TC, spin glass temperature Tg Susceptibility x (q), and retardation time τ using for born approximation and digamma function depend on wave vector(q) and cut off frequency(ω) in the region coexistence of superconductivity and spin glass in $Fe1+ySexTe_{1-x}$ compound.

Aim: To improve the coexistence of superconductivity and spin glass and *to* examine the associated Factor of electron doping and temperature in experimental and theoretical aspect of their coexistence.

Corresponding author: Anteneh Yesigat, Addis Ababa University, Addis Ababa, Ethiopia. Telephone +251-913-552086.

Keywords: coexistence, Superconductivity, spin glass, doping, susceptibility, ferromagnetism, Antiferromagnetism, pnictides.

Received: Sep 28, 2019 **Accepted:** Jun 02, 2020 **Published:** Jun 26, 2020

Editor: Muhammad Humayun, Huazhong University of Science and Technology, China.

Introduction

Superconductivity is a phenomena occurring in a certain materials at extremely low temperature, characterized by exactly zero electrical resistance as wall as there is no magnetic field. It was discovered in 1911 by Heike kamerlingh Onnes, who was studying the resistance of solid mercury at extremely low temperatures using the recently discovered liquid helium as a refrigerant. He found that DC resistivity of suddenly drops to zero below 4.2k and [2] observed that the resistance appropriately disappeared. Superconductivity has been found early in various elements such as mercury, lead, and aluminum. Most early superconductors are superconducting at extremely low transition temperature and low magnetic field.

In recently February 2008, Hideo Hoson(from the Tokyo Institute of Technology in Japan) has discovered an iron based superconducting material in LaOFFeAs (1111) family. The critical temperature for this iron arsenide compound with lanthanum, oxygen and fluorine is 26K. The general formula (1111) family RFeAsO where R-replaced by (R=La, Ca, Sm, Pr, Nd) and other rear earth elements. The corresponding elements increase the transition critical temperature markedly: 41K for Ce, 52K for Pr, 52K for Nd, and 55K for Sm. The Superconductivity has been also discovered in fluorine-free systems, including $RFeAsO1-X$ (R=La, Ce, Pr, Nd, Sm, Gd and TC value b/ n = 1K 55K), it was surprising that there could be another material other than the cuprites which could become superconducting an elevated temperatures.

The recent discovery of non-oxide superconductors in MgB_2 and iron-based compound RFeAsOF would also assist theoretical physicists to be closer to a fundamental understanding in the basic mechanism behind high temperature. In general, their on pnicide superconductor family has been quickly expanded to six different structures, and the superconducting transition temperature has been rapidly raised to approximately 57k.

Most physical properties of superconductors vary from material to material, such as the heat capacity, the critical temperature, critical current density, and critical field at which superconductivity is will differ. However, there is a class of properties that are not dependent of the mentioned material. For instance, all superconductors have exactly zero resistance and there is no internal magnetic field.

Interplay between superconductivity and magnetisms are interesting topic in condensed matter physics. The magnetic system exhibit different types of order depending on temperature (T), spin alignment based on external magnetic field (H) etc. In experimentally a magnetic material frustration in the spin of interaction that is called spin glass (S.G). Some properties of spin glass as following property can be shown that (i)low field low frequency a. susceptibility $Xa.c$(T) exhibiting a cusp of at temperature Tg, the cusp can get flatted at temperature cold for small magnetic field(H) as 50 Gauss.(ii)no sharp anomaly appears in the specific heat. (iii)AC susceptibility begins to deviate from the curie low at temperature $T>>Tg$, and soon. Superconductivity and ferromagnetism are often thought to be incompatible, according to BCS theory [5], a superconductor explains in a magnetic field, which in turn destroys superconductivity. However, both superconductivity and magnetic order has been seen in harmony (coexists) in some of rare-earth compound. The coexistence of superconductivity and ferromagnetism is quite peaceful and very weakly influences each other.

Mostly the superconductivity coexist with spin glass occur in(11) and(122)family, because they have vary at low critical temperature $Fe_{1+y}Se_XTe_{1-X}$ and $Ba(Fe_{1-y}Co_X)_2As_2$ there is evidence for coexistence of spin glass and superconductivity. In generally believed that magnetism play fundamental role in superconducting mechanism like other family, because superconductivity occurs when mobile electrons or holes are doped into anti-ferromagnetic elements like Te or Se parent compound. Experimentally has been revealed that superconductivity and spin glass coexist in Selenium (Se) and Tellurium (Te) iron pnictide compound of ($Fe_{1+y}Se_XTe_{1-X}$) with occur in the short range in the region of ($0.1 \leq X \leq 0.5$).

Background

A discovery of high temperature superconductivity in cuprate superconductors appears in twenty years ago. In the recent time the high temperature of superconductor un expected discovered based on Fe-Pnictides approximately six different

structures of the FeAs layer families have been found. They are 11, 111, 122, 1111, 32522, and 21311 (or 42622) families. Let see different families of Fe-pnictides.

1)1111family

The first discovery of high - T_C superconductivity in $RFeAsO_{1-X}F_X$ for (R=La, Sm, Ce, Nd, Pr), The critical temperature (*TC*) rapidly increased by exchanging lanthanum with rare earth ions of smaller atomic radii in LaFeAsO and appropriate carrier doping or creating oxygen deficiency. it reached a maximum value of ~ 56K until now in $Gd1-XThX$ FeAsO. This family LaFeAsO came to be known as 1111 family. Note that LaFePO, also discovered by Kamiara et al in 2006 was the first 1111 compound to show superconductivity, but with very low ($T_C \approx$ 5 - 7K). In addition to $LaFeAsO_{1-X}F_X$, the most remarkable 1111, compounds that Show high-*TC* superconductivity discovered until now are:

i) imFeAsO1−XFX(TC ≈ 43K)

ii) CeFeAsO1−XFX(TC ≈ 41K)

iii) NdFeAsO1−XFX(TC ≈ 51K)

iv) *PrFeAsO1−XFX(TC ≈ 52K)*

2)122 family

RFe_2As_2 for (R= Ba,Ca,Sc)BaFe2As2 as a potential new parent compound based on the similarities between BaFe2As2 and LaFeAsO. In fact, both compounds contain identical(FeAs) layers, and have the same charge accordance as follows: *Ba*2+ [(*FeAs*)].(*LaO*)+(*FeAs*). Partial replacement of Barium with Potassium (hole doping) induced superconductivity at 38K in $Ba_{0.6}K_{0.4}Fe_2As_2$, the first member of a new family of superconducting iron arsenide known as the 122 family. This discovery was followed by reports of similar compounds with:

i) Strontium (*TC* ≈ 37*K*)

ii) Calcium (*TC* ≈ 20*K*)

iii) Europium (*TC* ≈ 32*K*). Later electron doping in *BaFe*2*As*2 by the partial replacement of Fe with Co with *TC* ≈ 22*K* was reported by Se fat.

3)111 family

The discovery of another new superconducting iron arsenide system AEFeAs (AE = alkaline metal.) Superconductivity with *TC* up to18K was found in these compounds.

4)11 family.

The observation of superconductivity with zero resistance transition temperature at 8K in the PbO - type *α* - FeSe, compound known as11 family. Although FeSe has been studied quite extensively, a key observation is that the clean superconducting phase exists only in those sample prepared with intentional Se deficiency.

Crystal Structure of Fe pnictides

1111 family,

LaFeAsO (1111) family of iron pnictide crystallizes in the ZrCuSiAs- type structure, (space group P4/nmm). In this structure, two-dimensional layers of edge – sharing *FeAs* trihedral alternate with sheets of edge sharing *OLa* tetrahedral as shown below Figure 1(a). Because of the differences between the ionic nature of the La-O(Lanthanum oxide) bonds and the more covalent Fe-As (iron arsenide) bonds, a distinctive two-dimensional structure forms, where ionic layers of lanthanum oxide (LaO)+ alternate with metallic layers of iron arsenide (*FeAs*).

2)122 family

The ternary iron arsenide *BaFe*2*As*2, with the tetragonal *ThCr*2*Si*2 type structure space group (space group *I*4/*nmm*) contains practically identical layers of edge – sharing *FeAs*4/4 tetrahedral, but they are separated by barium atoms instead of LaO sheets. This structure is shown in Figure 1(b).

3)111 family,

LiFeAs crystallizes into a *Cu*2*Sb*-type tetragonal structure containing [FeAs] layer with an average iron valence *Fe*2+like those for 1111 or 122 parent compounds. This structure is shown in Figure 1(c).

4)11 family,

The PbO-type *and FeSe* crystal structure is shown in Figure 1(d). They have been particular interest the activity brining between the magnetic spin fluctuation and super-conductivity. When the anti-ferro magnetic(AFM) order associated with the Fe-X (X= As Te) layers is weakened by doping electrons or holes. Mostly occur in (1111) and (122) families, such as *SmFeAsO*1−*XFX* and *Ba*(*Fe*1−*XCoX*)2*As*2 there is evidence for coexisting anti-ferromagnetic order and superconductivity. The other situation different in the

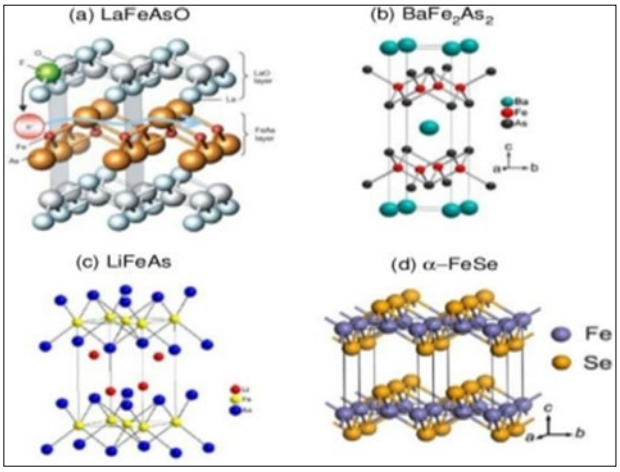

Figure 1. Schematic crystal structure of: (a) LaFeAsO, (b)$BaFe_2As_2$ (c) LiFeAs (d) FeSe.

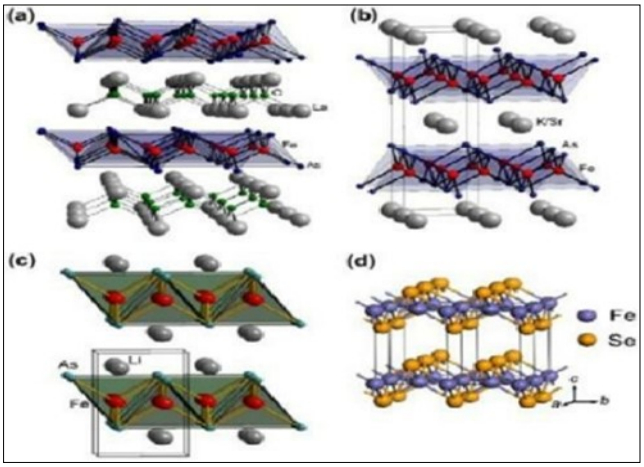

Figure 2. The four pnictide families currently known the superconductor occur the Fig (a, b, c) three metallic layers are FeAs but Fig(d) metallic layer in FeSe.

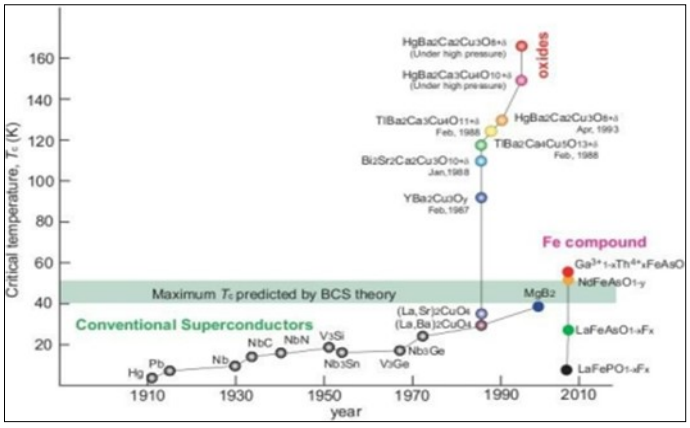

Figure 3. The time evolution of the superconducting critical temperature.

chalcogenides system in 11 family of $Fe1+ySeXTe1-X$ compounds. Here detail in sensitive to the Fe as well as Se concentration and we will focus on the situation for decrease excess Fe(*i.e.,* $y \approx 0$). The Neel temperature drops rapidly for $X = 0.1$, but our measurements indicate that bulk superconductivity only appears for $X = 0.4$.

We will present the $Fe1+ySeXTe1-X$ (FST) compound in magnetic and superconducting property as well as the coexistence of spin glass with superconductivity behavior in the short regime. (Figure 2)

High-Tc Superconductivity in Iron pnictide

High-Tc superconductivity at 26K was reported by Kamiharaetal. He was seen LeFeAsO (1111) family for doping of fluorine element to form $LeFeAsO_{1-X}F_X$ compound was formed. The high T_C superconductor is completely a new class in nitrogen family for Fe based compound is called iron pnictide. This was the discovery as generated agreat interest of material sciences community opening a new route for the high T_C in the Fe pnictide class. However, this has also brought new challenges on both experimental and theoretical side view. The scientists have a new problem for cuprate and ferro-pnictde materials. Let see LaFeAsO 1111 family compound dope electron transfer from oxygen to fluorine atom that compound change to $LaFeAsO_{1-X}F_X$ form. This is completely new class in creasing TC value, so this iron based compound is called iron pnictide. (Figure 3)

From the above figure see for the previous year conventional superconductor occur in heavy element like (Hg, Pb...) in the half century the compound form superconductor exist very high critical temperature. The compound that have CO_2 layer is called cuprate. Recently interesting study of superconductivity coexists with magnetism by exchange magnetic interaction and electron interaction study by BCS theory, the corresponding CO_2layer change to FeAs layer.

For the different family of Fe-pnictide has different T_C value. (Table 1)

Inter Relationship Existence of Fe- pnectied Cuprate

The electron sin Fe-pnictide are strongly correlated as cuprate, which surely in their parent and lightly hole doped state evidently behave Mott-insulator.

Important Similarity between Fe-pnictide and Cooperates.

1) Both arelayer system.
2) Both haved-electron playing a crucial role,
3) oth feature close proximity of AFM order and SC in respective phase diagram.

§ But there are critical difference as wall as.

1) The d-electroncountin Fe uses six (even) but Cu use nine (odd).
2) The parent state of a $CuO2$ layer can be modeled by asingle (hole) half-filled band and discovered band-structure theory should be good metal.
3) Cuprate are any thing but as their parent state is turned into Mott-insulter and Neel AFM by strong short-range coulomb repulsion U. Penalizes putting two electrons or holes in this case on the same site making it impossible to move the charge around in a (half-filled band) in the context having six d-electrons or four d-holes in a filled d-shell Fe-pnictide demand a multi-band description from the start.
4) Fe pnictide layer demand a multi-band description. It parent is semi-metal for several electron and hole pocket on Fermi surface defined as boundary b/n occupied state function of momentum. (Table 2)

Superconductivity in Meissner Effect

The Meissner effect was discovered in 1933 by Water Meissner and Robert Ochsn field[5]. It is one of the properties of superconducting materials. When a superconductor below critical temperature (Tc) is placed under a weak external magnetic field B, it repels the magnetic flux (field) B completely from its interior. It does this by setting up electric currents near it surface. It is the magnetic field of these surface currents that cancels out the applied magnetic field with bulk of superconductor. However, near to the surface distance called the London penetration depth. The magnetic field is not completely canceled; this region also contains the electric currents, whose field cancels the applied magnetic field with in the bulk superconductivity. This exclusion of magnetic flux from superconductor (B = 0) is known as Meissner effect.

Table 1. For Six different structures and typical superconductors are based on FeAs - system.

Families	**Formula**	***T_C* Value**
11	$Fe_{1+y}Se$, $FeTe_{1-x}Se_x$	8k
111	LiFeAs, NaFeAs	13k
1111, oxygen based	Electron doping $RE_{1-x}AE_xFeASO$	55 - 56K' 25K
1111, Florin Based	$AE_{1-x}RE_xFeAsF(AE = Ba, Sr, Ca)$	56 - 57k
122	$AE_{1-x}AL_xFe_2As_2AE(Fe_{1-x}TMX)_2AEFe_2AS_{2-x}P_x$	38K, 20-28K, 30K
32522	$Sr_3Sc_2O_5Fe_2As_2$	0k

Abbreviations: RE - rare earth; AE - earth; TM (3d, 5d) - transition metals; HP - high pressure.

Table 2. Summery of cuprate and Fe – pnictide materials.

	***CuO_2* Systems**	***FeAs* Systems**
Mother Compound	AFM order $T_N \sim 500K$	Structure phase change $T_S \approx 150$ *AFM* Order $T_N \sim$ 135K
Phase diagram	Carrier doping	Chemical Substitution pressure
Electronic state	Single band	Multi - band
SC order parameter	d - wave T_C = 135*K*	Extend $S \pm$ *wave* T_C = 57K
Pairing Glue	AFM interaction	Under debate??

Table 3. Chemical Compositions Superconducting Properties and Structural Characteristics for $FeSe_{1-x}Te_x$ Single Crystals

Starting Composition	**Crystal Composition**	***TC* On set**	**Δ *TC*(*K*)**
*FeSeTe*0.3	*FeSe*0.56 *Te*0.41	8.9	3.8
*FeSe*0.5 *Te*0.5	*FeSe*0.39 *Te*0.57	13.1	2.2
*FeSe*0.4 *Te*0.6	*FeSe*0.3 *Te*0.66	13.1	2.8
*FeSe*0.3 *Te*0.7	*FeSe*0.25 *Te*0.72	13.6	1.5
*FeSe*0.1 *Te*0.9	*FeSe*0.09 *Te*0.86	11.5	2.3

(Figure 4)

(CGS) $B = B_a + 4\pi M = 0$

$M/B_a = -1/4\pi$

(SI) $B = B_a + \mu_0 M = 0$ (1.0)

$M/B_a = -1/\mu_0 = -\epsilon_0 C^2$ (1.1)

The result B = 0 cannot be derived from the characterization of a superconductor as medium of zero resistivity. From Ohm's law, $E = \rho j$, we see that if the resistivity ρ goes to zero while current density (J) is held finite, E must be zero. By the Maxwell equation relation $dB/dt = \nabla \times E = 0$, so that zero resistivity implies dB/dt = 0. This argument is not entirely transparent, but the result predicts that the flux through the metal cannot change on cooling through the transition. The Meissner effect suggests that perfect diamagnetic is an essential property of the superconducting state.

General Overview of Superconductivity in Fe pnictide

Cuprate can be under stood with in the strong electron correlation picture with the valance electron of pnictide show more itinerant and good bond structure. The anti-ferromagnetic and superconductor in the Fe-pnictide are need to be considered including the three-dimensional electronic structure which is not the case of cuprate. Moreover, the Fermi surfaces of Fe pnictide in contrast with a single Fermi surface in cuprate and an unusual chemical potential shift in cuprate whose origin may be the strong electron correlation as compared with a simple rigid band-model shift in case of pnictide. The superconducting occur in the Fe-pnictide for differently physical and chemical property this pepper detailed in 11 compound family.

Superconductivity of $FeSe_{1-X}Te_X$ Compound

The family of Fe-based superconductor on FeSe has attracted extensive attention for similar to those FeAs layer mentioned above crystal structure in Figure 1d The FeSe superconducting transition temperature of Tc(~8*K*) exhibits a compositional dependence, decreasing for both under doped and over doped material as observed in the cuprate. When see Crystal structure does not have a separating layer in ferromagnetic. For (11) type pnictide the *TC* value around 8K. Superconductivity show only, when prepared with deficiency of selenium (Se) and substituting doping of electron from Tellurium (Te) element.

The PbO-type compound $FeSe_{1-X}Te_X$ in the region b/n x = 0 and x = 1 the Te doping concentration has an effect on superconductivity. It was found that superconducting transition temperature increases with Te doping maximum electron that reaching a maximum $Tc \sim 15K$ at about 50−70% substitution, and then decreases with more Te doping. For polycrystalline of FeSe and $FeSe_{1-X}Te_X$ sample compound can be also increase *TC* value with applying pressure. Superconducting phase transition has been found as high 27K at 1.5*GPa*, when we see in FeSe or $FeSe_{1-X}Te_X$ compound the transition temperature was improved to approximately 37K. The structural distortion change the lattice parameters without breaking magnetic symmetry, was reported and believed to have a strong correlation with the occurrence of superconductivity. This suggests that a detailed investigation of the magnetic and electronic behavior of these material that interplay with structural change.

$FeSe_{1-X}Te_X$crystal with Te doping ($x \geq 0.5$), although resistivity measurement show superconductivity with onset transition temperatures around 14K for b/n X = 0.5 and X= 0.7 the resistance did not zero down in crystals of X= (0.9, 0.75, 0.67, 1.0). Note that in polycrystalline sample with X= 0.9, there is also a nonzero residual resistance. The fact that the resistance does not completely reach zero indicate non uniform distribution of Se and Te, consequently low concentration of superconducting component in as grown crystal. The FeSe is also much easier to synthesize, since it *doesn't* include toxic arsenic.

For T_C values varies it depending on doping elements $FeSe_{1-X}Te_X$(Table 3)

Magnetic Correlation with Superconductor in $FeSe_XTe_{1-X}$ Compound.

We discuss the phase diagram of this compound *FeSeXTe*1 −*X* in 11 iron family. These compound forms with the largest amount of extra Fe observed near the Te rich side of the phase diagram. Initial measurement of the $Fe_{1+Y}Te_{1-X}Se_X$ compound show super-conductor with critical temperature at15K for $X \sim 0.5$, there exist for all value less than 0.5 but when the value of X near to Zero the superconductivity

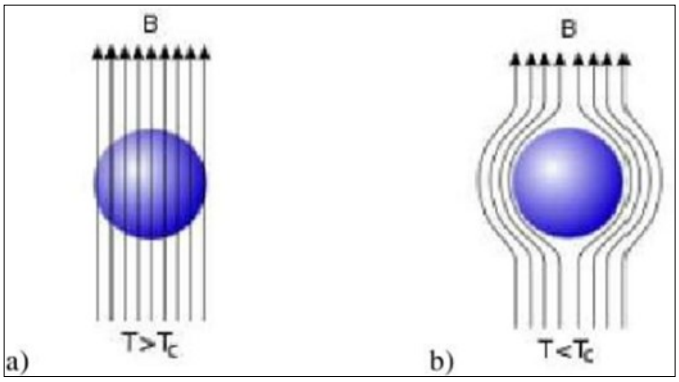

Figure 4. The Meissner effect. a)Magnetic field penetration above the critical temperature. b)Magnetic field penetration below the critical temperature.

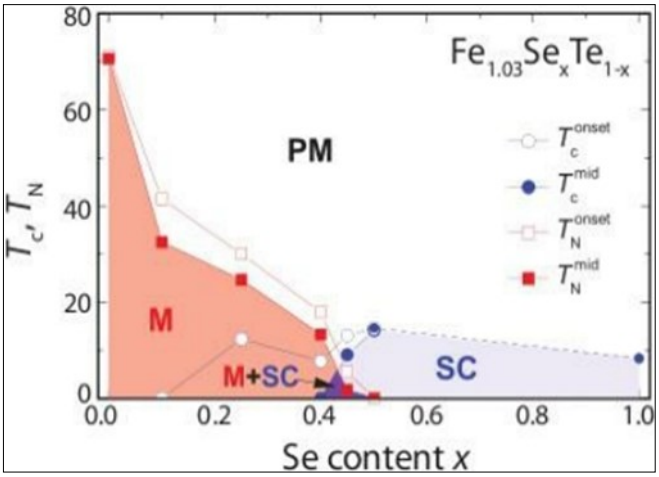

Figure 5. Experimentally determined phase diagram for $Fe_{1.03}Te_{1-x}Se_x$.

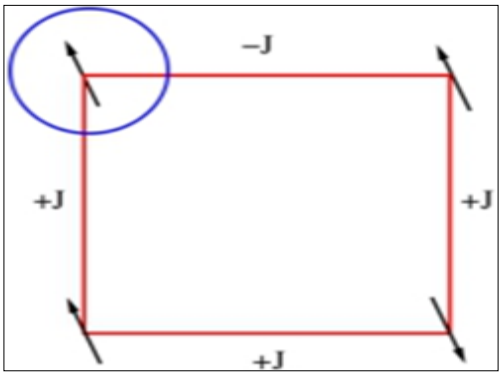

Figure 6. Illustration of frustration: The circled spin receives conflicting information from its neighbors and can point. Either up or down with the same energy. There is no ways can be reduced energy.

will be destroyed. Under this condition different phase diagram of superconductivity can be occurred. However, specific heat measurement in the single crystal that indicate bulk superconductivity for only concentration near to X = 0.5. From this circumstance, the phase diagram was investigated and indicated magnetic order for small value of X, which coexist with superconductivity over a range of concentrations in a manner very similar to the doped (122) and (1111) materials e.g $SmFeAsO_{1-X}F_X$. As mentioned previously, materials with low Se concentrations have a tendency to form with excess Fe to be measured the phase diagram with sample intentionally grown with Fe1.13\ at $y \sim 0.1$. It show an additional spin glass phase which coexist with superconductivity over much of measured Concentration range. This shows the sensitivity of these materials to stoichiometry and particular amounts of excess Fe present. (Figure 5)

Although, as discussed above there are some differences in the concentration dependent phase diagram of various Fe - based superconductor shows that there are some common features. All materials exhibita SDW state at low concentrations and this state is suppressed with doping allowing for the emergence of superconductivity. This show strong similarity with cuprate phase diagram.

The paramagnetic impurity of super conductivity is show the superconducting transition temperature was supposed by magnetic impurities. At some critical impurity concentration the transition temperature down to zero. Which gives an example of a quantum critical point? The critical concentration can be determined by this condition: $\tau_s\tau_{CO} = 2\gamma/\Pi$, where T_{CO} is the Superconducting transition temperature in a sample without impurity and τ_s the inverse proportion ($\tau \sim 1/n_s$)($n_s \sim 1/\tau_s$). It is the inverse life time spin-flip process for conduction electron. Note that the effect of the magnetic impurity on S.C is many aspects, similar to the one of the external magnetic field.

Theoretically We Can Distinguish Two Region.[19]

1) The first region above the concentration dependent magnetic critical temperature T_M, It means the transition of temperature from magnetic transition the assumption of non interacting magnetic impurities break down.
2) The second region of interest in $T<T_M$, where the interactions between magnetic impurities are strong and spontaneous magnetic ordering set in. There exists additional exchange field acting on the conduction-electron spin and conduction electron scattered by excitation of spin system. These additional mechanism lead to pair breaking in the superconducting state, for ferromagnetic ordering it is difficult to modify AG theory in this region to account for the magnetic interaction because of these additional mechanisms.

Spin Glass Magnetic Ordering

According to Edwards-Andersen model said that atoms are located on lattice point at regular intervals in a crystal. This is not the case in glass where the positions of atoms random in space. An important point is that in glasses the apparently random locations of atom do not change in a day or two in to another set of random locations. A state with the spatial randomness apparently does not change with time. The term spin glass implies that the spin orientation has been similarity to this type of location of atoming lasses: spin are randomly freezinging lass is called *spin glass*. Spin glasses are disordered or random solid state magnetic system in nonmagnetic host characterized by a random freezing of spin at rather well defined temperature *Tg*. It is the transition temperature exchange of impurity particle. However, it is very difficult to investigate the effect of single magnetic impurities experimentally based on measurement of sensitivity. In spin glasses the concentrations of the magnetic ion has to be small so the magnetic impurities substitute non-magnetic element at random position is known as QUENCHED, the other hand the crystallo-graphic disordering an inter metallic compound. This characteristic of spin glass system is known as Frustration. That able to detect the effects that need one needs a sufficient number of these impurities. It is also important to can beexist long-range interaction the magnetic spin is far apart between the (localized) impurities via the conduction of electrons.

The very important property of spin glass is their *unique nature* is the oscillating character of the exchange interaction. Because the randomly located spin that have interactions of essentially random sign, so that

spin glass is the peculiar (Douala) characteristics. The effective coupling between the magnetic moments can be either ferromagnetic or anti- ferromagnetic in short-range ordered is particularly favored energetic, it depend on the separation distance between two impurities. Consider the square lattices the two here (+) corresponds to $J > 0$ (Ferro) and (-) to $J < 0$ (anti- Ferro). Where, J exchanges interaction strength. The individual band energies are minimized if the two spins connected by any arbitrary bond ij are *parallel* to each other for $j > 0$ and anti parallel for $J < 0$. Now, since the impurities are randomly located within the crystal. The magnetic interactions are also randomly distributed. Thus the term spin glass is used in analogy with a real glass or an amorphous solid where the atoms are randomly distributed without any order or regular structure. (Figure 6)

The electrical resistivity, as well as the specific heat has been measured in the spin glass systems. From this measurement it has been found that a great deal of short-range magnetic clustering is already present at $T < Tg$. Such measurements establish beyond doubt that a majority of the spin participate in a local type of correlation. As temperature is lowered many of the randomly located, freely rotating spins come together by means of the correlation, into clusters that can then rotate as a whole. The remaining isolated spins are uncorrelated but serve to transmit interactions between the clusters. At $T = Tg$ these independent isolated spins freeze out in random directions.

Spin glass is rapidly developing aspect of solid which limit the usage of metallic alloys where long-range magnetic interactions are present. It is this long-range interaction (short-range interaction may also be present, through to a much smaller extent) that produces the random freezing of the spin moments a rather well defined temperature Tg, Short range and long range it depend on J_{ij} factor by r_i - r_j distance b/n neighbor s pin. $|J_{ij}| \rightarrow \infty$ for long range and $Jij \rightarrow 0$, Short range. We have also examined a variety of recent experiments performed on spin glass alloys with respect to three ranges of temperature $T > Tg$, $T = Tg$ and $T < Tg$. When $T > Tg$ *the* system usually occur in paramagnetic, $T < Tg$ is the magnetic susceptibility to be constant in the agreement in the experimental result and $T = Tg$ is not reel but on artifact the temperature depends on Q.

In the interpretation of the experimental behavior a phenomenological model is depending on the dynamically growing. It has been observed even at $T = Tg$ that some local correlations among the randomly separated spins also exist. The growth of magnetic clusters continues until $T \cong Tg$, when a few clusters above Tg clusters with more or less random spin directions are indicated by specific heat measurements, to fluctuate rapidly with time but instead are locked into random orientation.

The Random Spin Freezing Mathematically

$$\langle S_i \rangle_{\tau_0} = T_0^{-1} \int_0^{\tau_0} S_i(t)\, dt \qquad (1.3)$$

are non for some range of τ_0. Their mean square.

$$q(\tau_0) = N^{-N^{-1}} \sum_i \langle S_i \rangle_{\tau_0}^{\ 2} \qquad (1.4)$$

is this nonzero for some τ_0. The absence of *long – range* order and for a fixed impurity configuration we have, for $T > Tg$

$$\sum_i g_i \langle s \rangle_{\tau_0} \qquad (1.5)$$

Since the internal energy felt by a spin averages to zero if the (thermal) average is taken over a sufficiently long time where as for $T < Tg$ we have for spin glasses,

$$g_{ij} \langle S_i S_j \rangle = 0 \qquad (1.6)$$

Hence the spin glass order parameter is related to the above equation will give to Zero result.

$$|i - j| \rightarrow \infty \qquad (1.7)$$

Methodology and Experimental Views

Single crystals of $Fe1+ySeXTe1-X$ were grown by a modified Bridgman method as reported by neutron scattering. The neutron scattering measurements were carried out on triple- axis Spectrometer TASP at the spin Q installation source Paul Scherrer Institute in Switzerland. Bragg reflections from Pyrolytic Graphite PG (002) monochromatic and analyzer were used at a fixed at a fixed final wave vector of 2.66˚A. Pyrolytic Graphite filter was placed after the sample to reduce contamination from higher order harmonics in the beam and the instrument set up in the open collimation with the

analyzer focusing in the horizontal plane. The crystals were single rods with masses of approximately 4g. The magnetic excitations of the $Fe_{1+y}Se_XTe_{1-X}$ *are* magnetic and superconductivity in three phases.

The $Fe_{1.10}Se_{0.25}Te_{0.75}$ sample was orientated in two settings to give access to (*h, 0, l)* and (*h, k, 0*) planes in reciprocal space. Measurements of $Fe_{1.01}Se_{0.50}Te_{0.50}$ were made in the (h, k, l) plane only. In this report we index the reciprocal lattice with respect to the primitive tetragonal unit cell described by the P4/n mm space group with unit cell parameters $a \sim 3.8A^{\circ}$ and $C \sim 6.1A^{\circ}$ a long lines joining the nearest neighbor Fe atom.

Zero-field- cooled magnetization measurements were performed on a quantum design in MPMS magnetometer with a measuring field *H= 0.3m T*u sing the direct current method. That reduces to the effects of demagnetization, thin plate-like pieces of $Fe1+ySe_XTe1\text{-}X$ cleaved from the main single crystals. Zero-Field (ZF), Transverse Field (T_F), muon-spin rotation (μSR) experiments were performing on the three beam line. Transverse Field experiments a magnetic field of 11.8mT was applied parallel to the crystallographic the crystal and perpendicular to the muon-spin polarization.

The Neutron Scattering Experiments

The spin glass perform sat cold-neutron triple-axis spectrometer SPINS. Most of the experiments on the X= 0.15 and 0.3 single crystals were done with the instrument configuration of guide-open-80 open and energy of the scattered neutrons fixed to *Ef* =5meV. One be filter cooled by liquid nitrogen was placed after the sample for the elastic measurements. The X= 0.15 single crystal was aligned in the (h, k, 0) and the (h, 0, l) plane. High Q-resolution elastic measurement on the X= 0.1 and X= 0.15 single crystal ware performed using a back scattering geometry with energy *Ei* = 10*meV.* The neutron scattering experiment were determined the elemental concentration of electron in the crystal.

Mean-Filed Theory of Spin Glass

If the interactions between two spins are not uniform in the space, that interactions are ferromagnetic for some bonds and anti-ferro magnetic for other, than the spin orientation cannot be uniform in space, unlike the ferromagnetic system even at low temperatures. Under this circumstance it sometime happens that spins become randomly frozen-random in space but freeze in certain. This is the intuit picture of spin glass phase. It is applicable to the problem of disordered systems with random interaction . In particular we elucidate the properties so called replica systematic solution.

Experimental Properties of Spin-Glasses

Spin-glass behavior is usually characterized by AC susceptibility. The magnetic spins experience random interactions with other magnetic spins, resulting in a state that is highly irreversible and met a stable with realized below the freezing temperature (T_f) and the system is paramagnetic above this temperature. When above the freezing temperature ($T > T_f$) the system will be paramagnetic state (Figure 7)

The pressure (P) dependence of a.c susceptibility and electrical resistivity of $FeSe_{0.88}$ and $FeSe_{0.5}Te_{0.5}$ has been studied. The superconducting transition temperature (T_c) of $FeSe_{0.5}Te_{0.5}$ is found to be more sensitive to pressure than it is in $FeSe_{0.88}$, which is believed to a rise from the strongly distorted structure. The enhancement of(Tc) by (P) is mainly attributed to an increase of density of states, which implies that the superconductivity in $FeSe_{1-x}Te_x$ favors pairing mechanism in the context of strong-coupling in BCS theory. From the above figure has shown two characteristics of spin-glass. When the line sharp cusp at a temperature T_f this cusp indicate the a.c susceptibility is found to be an increasing function of concentration of the magnetic constituent in the alloy, it should be noted that for spin-glasses. In another said the line cusp flatted a temperature that means extremely depending on magnetic field. *At very low magnetic fields the corresponding to d.c magnetization depends on relaxation time. (τ).*This magnetic field cooled to the fill down up to zero cooled state. The a.c susceptibility measurement is the frequency dependence of T_f. It is found that T_f increases with ω (frequency).

The presence of large relaxation time of these samples was one of the first indicators that for these materials the coarse-phase space coordinates exhibits many valleys. Assume free energy of valley is as shown (Mean field theories also predict this but in this case in

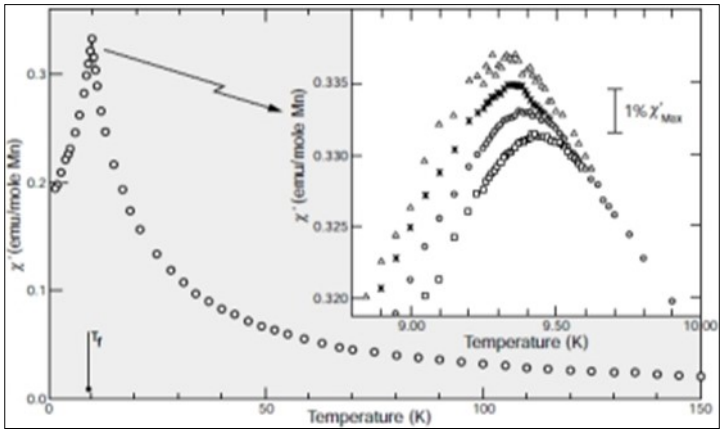

Figure 7. A.C susceptibility of CuMn (1at % Mn)showing the cusp at the freezing temperature. The frequency depend on the cusp from 2.6Hz (triangles) to1.33kHz (squares).

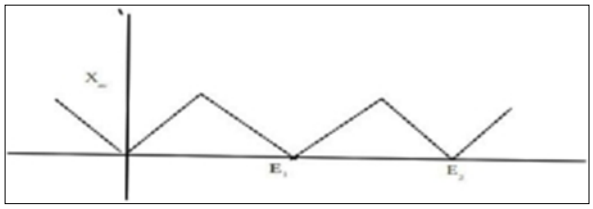

Figure 8. For free energy valley sharp cusp in the a.c susceptibility X_{ac}.

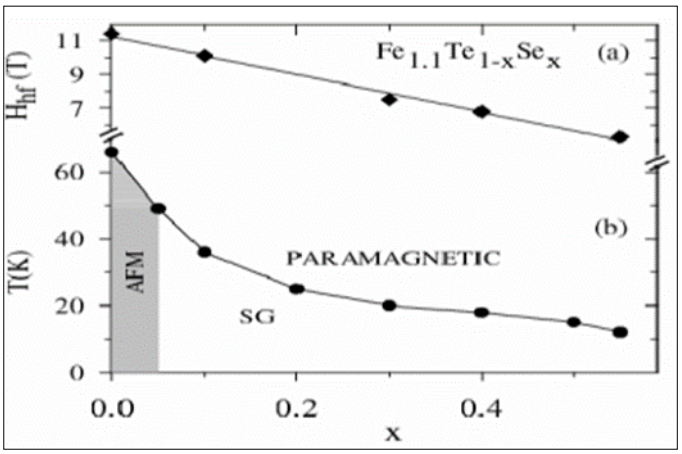

Figure 9. (a)Variation of average hyperfine field with Se concentration (b)Magnetic phase diagram

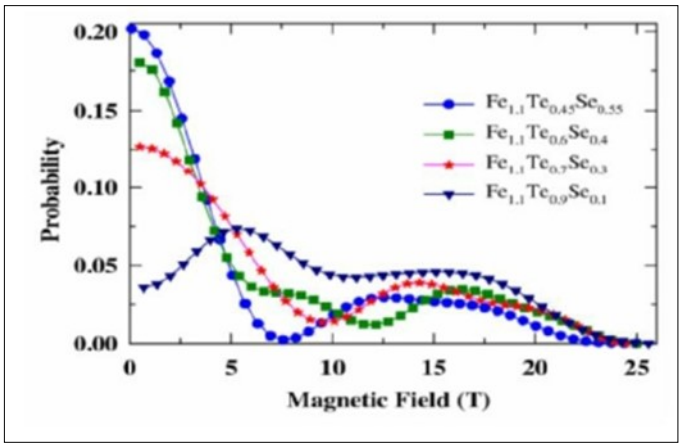

Figure 10. (color on line). Hyperfine field distribution from the Mssbauer spectra $Fe_{1.1}Te_{1-x}Se_x$ (x = 0.1, 0.3, 0.4, 0.55).

thermodynamics limit the height of the valley diverges. But for real systems it is finite) even though the presence of the sharp cusp in the a.c susceptibility. (Figure 8)

Prompted the experimental lists to propose the existence of a phase the transitionat T_f the specific heat measurement put some doubts in to the existence of the phase transition.

Coexistence of Magnetism, Spin Glass with Superconductivity

The Fe-pnictide or Chalcogenides is gradual emergence of the superconductivity when the anti-ferromagnetic (AFM) order associated with the Fe - X(X=Te/As) layers is weakened by doping $Fe_{1+y}Te$ has a tetragonal *α*-Pbo - type structure and forms only in the non stoichiometric form(Y in the range between 0.05 to 0.22) with the excess iron atoms Fe (2), occupying the octahedral positions in randomly. The Fe (2) directly couples to the four nearest neighbor but Fe (1) atoms in the Fe planes and could effectively introduce frustration in the under lying anti-ferromagnetic state. While $Fe_{1+y}As$ orders AFM, FeSe could be prepared in the stoichiometric form and is superconducting below 8K. Density functional theory suggests that FeSe could be an anti-ferromagnetic the bored line b/n *itinerant* and *localized* behavior and in plane Fe-Fe exchange coupling depend on Fe-Se distance. The doping concentration of electron $Fe_{1.1}Te_{1-X}Se_X$ (X = (0, 0.05, 0.1, 0.2, 0.3, 0.4, 0.5, 0.55 and 1) and $FeTe_{1-X}Se_X$(x = 0.1, 0.3, 0.4, 0.5) are prepare mixing Stoichiometric quantities of constitute element. Further increase of $Se(X > 0.1)$ in both $Fe_{1.1}Te_{1-X}Se_X$ and $FeTe_{1-X}$ series in superconductivity in temperature range 12k and 15k respectively. Because the superconducting transitions observed from the electrical resistivity and magnetic susceptibility in the $Fe_{1.1}Te_{1-X}Se_X$ (T_C) values well be less than $FeTe_{1-X}Se_X$ (T_C).

DC magnetization measurements in applied field of 0.5T investigation bulk magnetic order in these systems, For the *Fe*1.0 series, the Dc-magnetization is nearly constant above *TC* this implying that *Fe* is either no-magnetic or weakly magnetic property occur. This magnetization for the *Fe*1.1 series combine with Te to form $Fe_{1.1}Te$ compound sharply drops in below 65K. When the temperature freeze the magnetic order form in AFM exist the transition temperature of (T_{SDW}) 49K with doping X = 0 and 0.05 composition of electron. For X = 0.1. The magnetization shows broad maximum that progressively shifts to lower temperatures. This type of magnetization behavior is typical of spin-glass (SG) like system. This Spin glass nature is confirmed from sharp cusp in the *Xac* data, identified as the spin-glass temperature, *Tg*. The X_{ac} peak for X = 0.55 shifts to higher temperature eat higher frequencies proving the Spin glass nature beyond doubt. Magnetic field cooling effects are also observed below the spin glass transition temperature *Tg*. (Figure 9)

This phase diagram can assume a model where Fe(1) planes are made weakly magneticas result of Se substitution, while Fe(2) displays local magnetism and interacts with Fe(1), there by strongly influence the superconductivity cased by the Fe(1) there by strongly influence the superconductivity caused by the Fe(1) layer.Therefore Fe (2) interact magnetically and Fe (1) superconductivity in the $Fe_{1.1}Te_{1-X}Se_x$ series X $\geq$0.1.The Stoichiometric series in bulk superconductivity for X = 0.3, 0.4 and 0.5. The Fe Mossbauer live indicates no magnetic features down to 4.2K. The material depending on a. c susceptibility, this show magnetic and superconducting state in this case X= (0.3, 0.4 and 0.5). The diamagnetic screen corresponding to full X the heat capacity measurements do not show near *TC*, where as the curve showed stoichiometric series for X = (0.3, 0.4, and 0.5) the magnetic field of 14k, at this time the exponential drop indicating a Semiconductor energy gap is form superconducting state sample. (Figure 10)

The probability distribution of hyper fine field obtained. The distribution is very broad. The Hyperfine Mssbauer field is sensitive nature of the Fe. It is a local environment of this system. The distribution is nearly bi modal with a high field component centered on 15T possibly representing Se deficient neighborhood. The low field component is strongly enhanced by the Se substitution and this contribute factor emergence of competing magnetic interactions leading to the spin-glass state. The average hyperfine field (H_{av}) is found to drop linearly with the Se substitution (Figure 9) indicating that Se substitution gradually decreases the Fe moment, agreement with the bulk magnetization

data. Non-magnetic iron as if it were a magnetic hyperfine pattern with H_{av} < 4 Tesla. The magnetic fraction of Fe atoms are estimated from the hyperfine distribution range up to 4 Tesla.

The fractional values obtained are (0.75, 0.5, 0.43 and 0.32) for X= (0.1, 0.3, 0.4 and 0.55) respectively and it clearly exceeds Fe(2) fraction which is only 10%. This indicates that Fe(2) in the octahedral sites has strong direct, magnetic coupling with the Fe(1) in the planes.

The progressive reduction in the magnetic fraction of the Fe atoms canbe linked to the reduction of *μef f* with the

Substitution of Selenium (Se) from Tellurium (Te).

Coexistence Anti-Ferromagnetic, Spin Glass and Superconducting in Phase Diagram

In $Fe_{1+y}Se_XTe_{1-X}$ with 0.25 ≤ X ≤ 0.33 static, but short-range in commensurate magnetic order with *Qm* = (0.5 ± δ, 0.5 ∓ δ, *l*) is observed. [38, 44, 45] At higher Se concentration X ≥0.4 bulk superconductivity is achieved. The spin resonance energy at hω ≈ 6.5meV appears at incommensurate Q_c = (0.5 ± δ, 0.5 ∓ δ, *l*) [46, 47] The reduction in crystallographic symmetry important for magnetic ordering in *Fe*1+*yTe*. The monoclinic (orthorhombic) structure provides the magnetic ordering wave vector with a unique orientation with in the Fe planes. In the short – range magnetic order observed at $X \sim 0.3$ occurs in a tetragonal phase. It has two degenerate orientation for *Qm,*. This suggests that computation among degenerate domains may lead to frustration and keep the ordering SR.) The exchange interaction J_{ij} on the H= $\sum J_{ij} S_i.S_j$ is called SR and LR it depending on strength of exchange interaction in the separation distance between the spins.[22] A recent study has shown that Long Range the magnetic order for X ~ 0.075, thus might expect transition to short range SDW order for $X = 0.1$ and the long range Exchange interaction *Jij* on $Fe_{1+y}Se_XTe_{1-X}$ (FST) for X= 0.1 and 0.15 present that evidence of[17]

1)For magnetization measurement.

2)Characterizing short range order with neutron scattering. (Table 4)

$Fe_{1+y}Se_XTe_{1-X}$ (FST) and nature of magnetic correlations in three Non-superconducting samples of ($Fe_{1.01}Se_{0.1}Te_{0.9}$, $Fe_{1.01}Se_{0.15}Te_{0.85}$ and $Fe_{1.01}Se_{0.3}Te_{0.7}$).In that main result is the short range order is structural as well as magnetic consistent with present that orbital ordering is an important part of the magnetically ordered state.

At low energy *QC* spin fluctuation for X= 0.15 and X= 0.3 with in elastic neutron-scattering. While there is some weak critical scattering that extends out to *QC* near the onset of elastic scattering that disappears at low temp, as spin fluctuation are dominantly associated with *Qm*. These appear to be a broad spin glass (SG) in (FST). The critical changes in the Fermi surface (FS) doping on set of superconductivity and magnetism are competing state in the FeAs superconductors. (In the presence of the whole pockets S.C is fully suppressed, while in their absence the two states can coexist). $X \sim 0.1$ and might expect a transition to short range SDW occur.

For bulk magnetization measurements 0.01g single crystals with various Se concentration from X= 0 to X= 0.7 were used superconducting quantum interface device (SQUID) magnetometer, while for neutron measurement. The bulk magnetic susceptibility data obtained from single crystal of FST with four different Se - concentrations X= (0.04, 0.15, 0.3 and 0.5).(Table 5)

In neither spin glass case second order phase with neither observable long-range structural phase transition nor superconducting phase transition for doping Se to become superconductor. The set of bulk superconductivity appears to be associated with an evolution of characteristic with the spin fluctuation. For bulk magnetization measure (0.019), this single crystals various Se concentration for X = (0 - 0.7). (Table 6)

The X-T phase diagram for (FST) based on the bulk susceptibility obtained from the single crystal sample. Even though the values of X and Y are normal values or may not be exactly correct. The phase diagram clearly shows the trends and the existence of three distinct phases. When the $X \sim 0.1$ the anti-ferromagnetic phase but $X \sim 0.4$ the bulk Superconducting phase occurs and between the two regions the SG phase can be occur. (Figure 11)

In the spin glass compounds the transition is

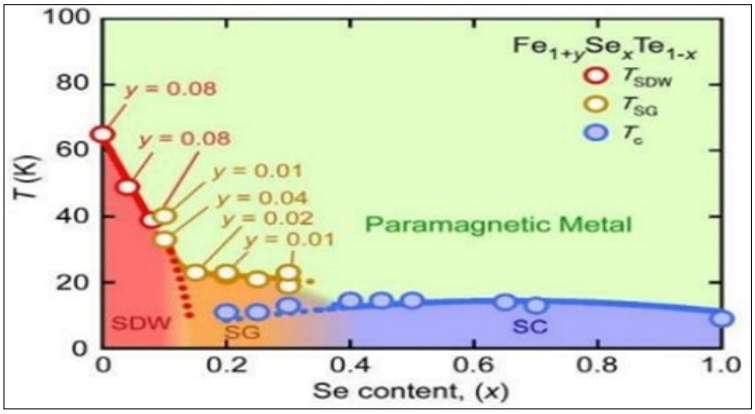

Figure 11. Phase diagram of $Fe_{1+y}Se_XTe_{1-X}$ with Y~0 as a function of X and T constructed from single crystal bulk susceptibility data some of which are shown in except for X = 1. The nominal Fe content Y = 0 unless it is specified. Tc (blue circles) represents the superconducting on set temperature.

Table 4. The magnetic order dependence on number of doping (hole or electron)

Compounds	**X - doping Value**	**Description**
Fe1+ySe0.75Te0.25,	*X*=0.75 and	It show among degenerate domains may be lead to frustration.
Fe1+ySe0.10Te0.9	*X* = 0.1	It keeps to ordering short range.
Fe1+ySe ≤ 0.075Te ≥ 0.025	*X* ≤ 0.075	With long range magnetic order
Fe1+ySe ≥ 0.1Te ≤ 0.9	*X* ≥ 0.1	A transition to Short-Range *SDW*-order,
Fe1+ySe≤ 0.075Te ≥0.025	At *X*= 0.1and *X*= 0.15	We show that spin-glass like behavior is present FST.

Table 5. Bulk magnetization is dependence on number of doping (hole or electron)

Compounds	**X- doping Value**	**Bulk Magnetization**
$Fe_{1.01}Se_{0.1}Te_{0.9}$,	*X* = 0.1	0.39 g
$FeSe_{0.15}Te_{0.85}$	*X*= 0.15	10.1 g
$Fe_{1.01}Se_{0.3}Te_{0.7}$	*X* = 0.3	5.3 g

Table 6. The freezing [63, 64] process $Fe_{1+y}Se_XTe_{1-X}$ from High T_C

No of X-doping Value	**The transition temperature**	**Indicating and description**
X = 0.04	At T_{SDW} = 49*K* (sharply decrease)	A long-range magnetic order.
X= 0.15 and 0.3	T_{Stt} ~ *23K*(by *Fc–ZFC* Below hysteresis)	A short-range magnetic order.
X=0.5	T_C =14.5*K*	The superconducting phase transition.

second order with neither observable long-range structural phase transition nor superconducting transition upon doping Se become superconducting. The X–T Phase diagram for FST based only on the bulk superconductivity data obtained from the single crystal samples X and Y are normal integral value may not exactly correct see the above table. The phase diagram can be experienced the long-range in SDW is non – Superconductor and the intermediate phase, some sample should partially superconductor below T_C ~ 11K, while other was non-superconducting down to1.4k. Some process to seen the spin glass form and coexist with superconductor, Firstly investigate the crystal structure at Low temperatures in the Spin-glass phase. We take performed high Q - resolution elastic measurement on X = 0.1 and X = 0.15 single crystals. When the low temperature barding that the structural tendency toward slower symmetry. The same scans were done at several different temperatures that data fit to a single Gaussian. The structural modification develops below 40k and weakness with increasing Se concentration.

Secondly, the static spin correlations in the spin glass phase were investigated using elastic Neutron scattering. The scans on X = 0.15 at 1.5k static magnetic peaks at incommensurate wave vectors Q = (0.46, 0, l+0.5) for integer of l. On cooling from higher temperature the static spin correlations gradually freeze below T_f= 40K. The increase of spin correlations coincides with the reduction in the intensity of the low energy excitation. The T_f measured by elastic neutron scattering with an energy resolution of ΔE ~ 0.3*meV* is higher than the T_{SG} measured by static bulk susceptibility, which is common in system involving spin freezing.

Mathematical Used to Solve of Problem

To study the coexistence of superconductivity and spin-glass (SG) in $Fe1+ySexTe1-x$ calculate of the time dynamics into the flip scattering time τ. This gives an approximation introducing the effect to dynamics on the pair breaking. While realize that it is only an approximation, It should be consider to complete solve the problem. The Born approximation is used to the spin-boson model in Ohmic regime.

The expression for $1/\tau$ in first born approximation contains the spin-spin correlation function, near *TC* the dominant contribution comes from long – range fluctuation. Using born approximation is $\psi k(r) \approx \emptyset_k(r)$.

First Born Approximation

$$\Psi_k(r) \approx \Phi_k(r) + \frac{2m}{h^2}\int d^3r' G_k^{\dagger})V(r')\Phi_k(r')$$

A way to motivated this to note that if we substitute the integral equation in to itself.

$$\Psi_k(r) \approx \Phi_k(r) + \frac{2m}{h^2}\int d^3r' G_k^{\dagger}(r,r')V(r')\Phi_k(r') + (\frac{2m}{h^2})^2 \iint d^3r'^3 G_k^{\dagger}(r,r')V(r')G_k^{\dagger}(r,r')V(r'')\Psi_k(r'^3) \quad (2.1)$$

We see that approximation, introduce error order V^2 this term is likely to be sub-dominate, We can write.

$$\Psi_k(r) \approx \frac{1}{(2\pi)^{3/2}} e^{ikr} - \frac{2m}{h^2}\frac{1}{4\pi}\frac{e^{ikr}}{r}\int \frac{d^3r'}{(2\pi)^{3/2}} e^{i(k-k_{out})\cdot r'} V(r') \quad (2.2)$$

So that

$$f(k,k_{out}) = \frac{-m}{(2\pi)h^2}\int d^3r'.e^{i(k-k_{out})\cdot r'}.V(r')\,. \quad (2.3)$$

Which we recognize as being $q = k - kout$, Where q is wave vector.

$$q^2 = k^2 + k_{out}^2\cos\theta = 2k^2(1-\cos\theta) = 4k^2 sin^2(\frac{\theta}{2}) \quad (2.4)$$

Second Born Approximation

The once more them the first $\psi k(r) \approx \varphi k(r)$ only at the second ,km \

$$\Psi_k(r) \approx \Phi_k(r) + \frac{2m}{h^2}\int d^3r' G_k^{\dagger}(r,r')V(r')\Phi_k(r') + \int\int d^3r'^3 G_k^{\dagger}(r,r'V(r')G_k^{\dagger}(V(r'\Phi_k(r')) \quad (2.5)$$

The Digamma Function

The definition of D.F is the logarithmic derivative of the Gamma function.

$$\Psi(z) = \frac{d}{dz}\ln\Gamma(x) = \frac{\Gamma(x)}{\Gamma(x)} \quad (2.6)$$

This is continuous except for the poles at zero and the negative integers, we can use the expression of the digamma function.

$$\Gamma(z) = e^{-\gamma z}\frac{1}{2}\prod_{K=1}^{\infty}\frac{e^{z/k}}{1+\frac{z}{k}} \quad (2.7)$$

Where γ is the Eular - Mascheron constant, and thus

$$\ln\Gamma(z) = \ln\left[e^{-\gamma z}\frac{1}{2}\prod_{K=1}^{\infty}\frac{e^{z/k}}{1+\frac{Z}{K}}\right]$$

$$= -\gamma z - \ln z + \sum_{k=1}^{\infty}\ln\left[\frac{e^{z/k}}{1+\frac{Z}{K}}\right]$$

$$= -\gamma z - \ln z + \textstyle\sum_{k=1}^{\infty}[\frac{z}{k} - \ln\left[1+\frac{z}{k}\right] \quad (2.8)$$

Taking the derivative with respect to z, we get

$$\Psi(z) = -\gamma - \frac{1}{z} + \sum_{k=1}^{\infty}[\frac{1}{k} - \frac{1}{z+k}]$$

$$= -\gamma + \textstyle\sum_{k=1}^{\infty}[\frac{1}{k} - \frac{1}{z+k-1}] \quad (2.9)$$

Now, immediately what happens if Z is a positive integer: the terms?

1/(n+k-1)

K=1, 2, 3, 4.....Canceled by the terms 1/k for k = n, n+1, n+2 ……..thus

$$\textstyle\sum_{k=1}^{\infty}[\frac{1}{k} - \frac{1}{z+k}] \quad (2.10)$$

And

$$\Psi_0(n) = -\gamma + \textstyle\sum_{k=1}^{\infty}\frac{1}{k} = -\gamma + H_{n-1} \quad (2.11)$$

And also we see immediately that $\psi 0$ (1) = -y and $\psi 0$ (2) =1-y (and thus only positive Zero of $\psi 0$ use b/n these two values) Using the series form,

$$\Psi_0(z) = -\gamma + \textstyle\sum_{k=1}^{\infty}\frac{1}{k} - \frac{1}{z+k-1} \quad (2.12)$$

We use

$$\Psi(z+1) = -\gamma + \textstyle\sum_{k=1}^{\infty}\frac{1}{k} - \frac{1}{z+k} \quad (2.13)$$

And

$$\Psi(z+1) - \Psi_0(z) = -\gamma + \sum_{k=1}^{\infty}\frac{1}{k} - \frac{1}{z+k} + \gamma - \sum_{k=1}^{\infty}\frac{1}{k} + \frac{1}{z+k}$$

$$= \textstyle\sum_{k=1}^{\infty}(\frac{1}{z+k-1} - \frac{1}{z+k}) \quad (2.14)$$

$$= 1/z$$

$$\Psi(z+1) = \Psi_0(z) + \frac{1}{z} \quad (2.15)$$

As recurrence relation for ψ_0, now recall the Euler-reflection formula we derived previously.

$$\Gamma(z)\Gamma(1-x) = \frac{\pi}{\sin\pi x} \quad (2.16)$$

Taking the logarithm of both said, and differently.

$$\ln\left(\Gamma(z)\Gamma(1-x)\right) = \ln\frac{\pi}{\sin\pi x}$$

$$\ln\Gamma(z) + \ln\Gamma(1-x) = \ln\frac{\pi}{\sin\pi x}$$

$$\Psi_0(x) - \Psi_0(1-x) = -\pi\cot(\pi x) \quad (2.17)$$

Applying a similarly Legendre duplication form.

$$\Gamma(2z) = \frac{2^{2x-1}}{\sqrt{\pi}}\boldsymbol{\Gamma}(\boldsymbol{z}+\tfrac{1}{2})\boldsymbol{\Gamma}(\boldsymbol{z})$$

$$\ln\Gamma(2z) = (2z-1)\ln 2 - \frac{1}{2}\ln\pi(z) + \boldsymbol{\Gamma}(\boldsymbol{z}+\frac{\boldsymbol{1}}{\boldsymbol{2}})$$

$$2\Psi_0(2z) = 2ln2 + 2\,\Psi_0(z) + \Psi_0\left(z+\frac{\boldsymbol{1}}{\boldsymbol{2}}\right)$$

$$\Psi_0(2z) = \frac{1}{2}\Psi_0(z) + \frac{1}{2}\Psi_0\left(z+\frac{\boldsymbol{1}}{\boldsymbol{2}}\right) + ln2$$

Put in z=1/2 ,in to eqn(2.1.16) we can get

$$\Psi_0(1) = \frac{1}{2}\Psi_0\left(\frac{1}{2}\right) + \frac{1}{2}\Psi_0(1) + ln2$$

$$\Psi_0(1) = \frac{1}{2}\Psi_0\left(\frac{1}{2}\right) + 2ln2$$

$$\Psi_0\left(\frac{1}{2}\right) = \Psi_0(1) - 2ln2$$

$$\Psi_0\left(\frac{1}{2}\right) = -\gamma - 2ln2 \quad (2.18)$$

Theoretical Formulation

The model Hamiltonian for coexistence Spin glass Superconducting in the compound of ($Fe_{1+y}Se_xTe_{1-x}$) and ($Fe1-xCox)_2As_2$) our system can be described as:

$$H = H_{intra} + H_{inter} \quad (3.1)$$

$$H_{intra} = H_{BCS} = \sum_{p\delta}\epsilon_p\, c^{\dagger}_{p\delta}c_{p\delta} - V\sum_{kk}\hat{c}^{\dagger}_{p\uparrow}\hat{c}^{\dagger}_{-p\uparrow}\hat{c}_{-p\downarrow}\hat{c}_{p\downarrow}$$

$$H_{inter} = -\frac{1}{2}\sum_{i,j,\delta,\delta'\delta}e^{i(k-k')}\left[\vec{S}_i\left(C^{\dagger}_{k\delta}\sigma_{\sigma\sigma'}C_{K\sigma'}\right)\right] - \frac{1}{2}\sum_{ij}J_{ij}\,\vec{S}_i\vec{S}_j$$

Where H_{BCS} is the BCS Hamiltonian for the system without magnetic impurities, (σx, σy, σz) are the three

Pauli matrices and *Si* magnetic spin located at *Ri*, It is the s-f block exchange term and J_{ij} is the exchange interaction. The second term describes the interactions between the electrons and the localized spins of rare-earth(R) or transition metal ion while the third term describes the interactions b/n localized spins. The coupling lead to magnetic ordering at temperature T_M the concentration of magnetic impurities X.

A brikosov' and Gorkovisos first show that is the born approximation *TC* is given by:

$$\ln\frac{T_C}{T_{CO}} = \Psi_0(1/2) - \Psi_0\left[\frac{1}{2} + \frac{1}{2\pi T_{C\tau}}\right] \quad (3.2)$$

Applying the above expression for the diagram for using $\psi(z)$ is digamma function, for z = 1/2, than recall the digamma function.

$$\Psi_0(1/2) = -\gamma - 2\ln 2 \quad (3.3)$$

And

$$\Psi_0\left[\frac{1}{2} + \frac{1}{2\pi T_{C\gamma}}\right] = \Psi(Z + \frac{z}{\pi T_{C\gamma}}) \quad (3.4)$$

For z=1/2 and that m=1/πT$_{Cv}$

$$\Psi(Z + Zm) = -\gamma + \sum_{k=1}^{\infty}\left[\frac{1}{k} - \frac{1}{z+zm+K-1}\right]$$

$$= \Psi(z) + \sum_{k=0}^{\infty}\left[\frac{1}{k} - \frac{1}{z+zm+K-1}\right] - \left[\frac{1}{k} - \frac{1}{z+zm+K-2}\right] \quad (3.5)$$

$$\Psi(Z + Zm) - \Psi(z) = \sum_{k=0}^{\infty}\left[\frac{1}{k} - \frac{1}{z+zm+K-1}\right] - \left[\frac{1}{k} - \frac{1}{z+zm+K-2}\right]$$

$$\psi(Z+Zm) - \psi(z) = 1/(zm-1) - 1/(zm+1) \quad (3.8)$$

Combining the two equations, we can get

$$\Psi(Z + Zm) = \Psi(z) + \frac{1}{zm-1} - \frac{1}{zm+1}$$

Than substitute the value of Z=1/2 and M=m+1, and m=1/πT$_{Cv}$

$$\Psi\left[\frac{1}{2} + \frac{1}{2\pi T_{C\gamma}}\right] = \Psi\left(\frac{1}{2}\right) + \frac{2}{(zm)^2-1} \quad (3.9)$$

Recall from eqn (3.1.2)

$$\ln\frac{T_C}{T_{CO}} = \Psi(\frac{1}{2}) - \Psi\left[\frac{1}{2} + \frac{1}{2\pi T_{C\tau}}\right]$$

$$= \Psi\left(\frac{1}{2}\right) - \Psi\left(\frac{1}{2}\right) + \frac{8}{M^2-4} = \frac{8}{\ln(\frac{T_C}{T_{CO}})}$$

Re arranging the above equation is gives

$$\tau = \frac{1}{\pi T_C}\left[\left(\frac{8}{\ln\left(\frac{T_C}{T_{CO}}\right)} + 4\right)^2 - 1\right]^{-1} \quad (3.10)$$

Take the value of *TC*0=8k, and *TC*=14.5K value of this compound $Fe_{1.1}Se_xTe_{1-x}$ for we can get

$$\tau = \frac{1}{3.14*14.5}\left[\left(\frac{8}{\ln\left(\frac{14.5}{8}\right)} + 4\right)^2 - 1\right]^{-1} \quad (3.11)$$

Than τ = 0.006912, the spin flip scattering time, When the spatial and time correlations are taking the result. For τ can be generalized within born approximation.

$$\frac{1}{\tau} = \frac{1}{\tau_{AG}}\frac{1}{2K_F^2\,S(S+1)}\int^{2K_F} qdq\int_{-\infty}^{\infty} d\omega g(q,\omega)\frac{\beta\omega}{e^{\beta\omega}-1} \quad (3.12)$$

Where

$$g(q,\omega) = S(q,\omega) - S_{Bragg}(q,\omega) \quad (3.13)$$

And

$$S(q,\omega) = \frac{1}{2\pi N}\int_{-\infty}^{+\infty} dt \sum_{ij}\langle S_i(t)S_j(0)\rangle e^{iq.R_{ij}}$$

$$S_{Bragg}(q,\omega) = \frac{1}{2\pi N}\int_{-\infty}^{+\infty} dt \sum_{ij}\langle S_i(t)S_j(0)\rangle e^{iq.R_{ij}}$$

This result for $1/\tau = 1/\tau Att$ in the limit $S(q,\omega) \sim \delta(\omega)\delta(q)$,

$$g(q,\omega) = \frac{K_\beta T}{q^2\mu^2}(X(q))(\frac{\beta\omega}{e^{\beta\omega}-1})F(q,\omega) \quad (3.14)$$

Insert eqn (3.0.14) in to eqn(3.0.12), we can get

$$\frac{1}{\tau} = \frac{1}{\tau_{AG}}\frac{1}{2K_F^2\,S(S+1)}\int^{2K_F} qdq\int_{-\infty}^{\infty} d\omega\,\frac{K_\beta T}{q^2\mu^2}(X(q))(\frac{\beta\omega}{e^{\beta\omega}-1})\frac{Dq^2}{\pi(Dq)^2+\omega^2} \quad (3.15)$$

$$\frac{\tau_{AG}}{\tau} = \frac{K_\beta T}{\tau_{AG}}\int^{2K_F}\frac{q*D}{T-T_M+a^2q^2}dq\int_{-\infty}^{\infty} d\omega\,(\frac{\beta\omega}{e^{\beta\omega}-1})\frac{1}{\pi(Dq)^2+\omega^2}$$

For the power series expansion.

$$e^{\hbar\omega} - 1 = 1 + \beta\omega + (\beta\omega)^2 + (\beta\omega)^3 + \cdots - 1 = \beta\omega \quad (3.16)$$

So that

$$\frac{\beta\omega}{e^{\hbar\omega}-1} = 1$$

$$\frac{\tau_{AG}}{\tau} = \frac{1}{2K_F^2}\int^{2K_F} qdq \int_{-\infty}^{\infty} d\omega \frac{K_\beta T}{q^2\mu^2}\left[\frac{1}{T-T_M+a^2q^2}\right]\frac{Dq^2}{\pi(Dq)^2+\omega^2}$$

$$\frac{\tau_{AG}}{\tau} = \frac{K_\beta T}{2K_F^2}\int^{2K_F} \frac{q*D}{T-T_M+a^2q^2}dq \int_{-\infty}^{\infty} d\omega \frac{1}{\pi(Dq)^2+\omega^2}$$

We assume that the spin-diffusion constant D

$$D = D_0(T/T_g - 1 + (aq)^2)^{1/4} \quad (3.17)$$

$$\frac{\tau_{AG}}{\tau} = \frac{K_\beta T}{2K_F^2}\int^{2K_F} \frac{q*D}{T-T_M+a^2q^2}dq\left[\frac{1}{\pi}*\pi\right]$$

Integrate above equation we obtain and

$$\frac{\tau_{AG}}{\tau} = \frac{K_\beta T}{2K_F^2}\int^{2K_F} \frac{q*D}{T-T_M+a^2q^2}dq$$

$$\frac{\tau_{AG}}{\tau} = \frac{K_\beta T D_0}{2K_F^2\mu^2}\int^{2K_F} \frac{q*(T/T_M-1+a^2q^2)^{1/4}}{T-T_M+a^2q^2}dq \quad (3.18)$$

For approximation the two terms.

$$\frac{\tau_{AG}}{\tau} = \frac{K_\beta T D_0}{2K_F^2\mu^2 T_a}\int^{2K_F} \frac{q}{T-T_M+a^2q^2}dq$$

$$\frac{\tau_{AG}}{\tau} = \frac{K_\beta T/T_g D_0}{2K_F^2\mu^2}\left[\frac{1}{a^2}(T/T_M-1+(2K_F)^2a^2)^{1/4}\right] \quad (3.19)$$

We take the Brillouin zone wave vector = 2*KF*, we can simplify to get and Where the constant value take

$$C = \frac{K_\beta D_0}{K_F^2\mu^2a^2}, \quad E = \frac{q^2a^2}{T_{CO}}$$

$$\frac{\tau_{AG}}{\tau} = C\left[(T/T_M - 1 + ET_{CO})^{1/4}\right] \quad (3.20)$$

If the ω dependence of $g(q,\omega)$ is purely elastic, we obtain the expected behavior of $1/\tau$ expressing more in this equation,

$$g(q,\omega) = \frac{K_\beta D_0}{K_F^2\mu^2a^2}X(q)\frac{\beta\omega}{e^{\hbar\omega}-1}F(q,\omega,) \quad (3.21)$$

Where x(q) is the q-dependent susceptibility and $F(q,\omega)$ is the spectral weight function, since

$$F(q,) = \frac{1}{\pi}\frac{Dq^2}{(Dq^2)^2+\omega^2} \quad (3.22)$$

Where, D is the spin-diffusion constant.

$$X(q) = \frac{q^2\mu^2}{K_\beta T}\frac{e^{\beta\omega}-1}{\beta\omega}\frac{g(q,\omega)}{F(q,\omega)}$$

$$= \frac{q^2\mu^2}{K_\beta T}\frac{e^{\beta\omega}-1}{\beta\omega}\frac{\frac{1}{2\pi N}\left[\int_{-\infty}^{+\infty} dt\, e^{-i\omega t}\sum_{ij}\left[\langle S_i(t)S_j(0)\rangle e^{ir.R_{ij}} - \langle S_i\rangle\langle S_j\rangle e^{ir.R_{ij}}\right]\right]}{\frac{1}{\pi}\frac{Dq^2}{(Dq^2)^2+\omega^2}}$$

Rearrange the above equation using power series for ferromagnetic case eqn (3.0.16) assume or stein-Zernike form can we get

$$X(q) = \frac{S(S+1)}{T-T_g+a^2q^2} \quad (3.23)$$

We tried different form for D, including D constant and find that the results for $1/\tau$ and the phase diagrams are essentially insensitive to the T and q-dependence of D. When the spin – fillip scattering rate form

$$\tau_0\tau_S n_s = \frac{1}{4\pi^2S(S+1)} \quad (3.24)$$

When the spin of magnetic impurity $\tau_s \sim \tau_{AG}$ τs eqn (3.24) we can get

$$X(q) = \frac{1}{T-T_g+a^2q^2} * \frac{1}{4\pi^2\tau_0\tau_S n_s} \quad (3.25)$$

From RKKY interaction radiation system theory the spin glass transition $Tg \sim \tau_{ons}$

$$X(q) = \frac{1}{4\pi^2\tau_0\tau_S(T-T_g+a^2q^2)}$$

$$= \frac{1}{4\pi^2\tau_0\tau_S(T-T_g+ET_{co})}$$

$$X(q) = \frac{1}{4\pi^2\tau_0\tau_S(\frac{T}{T_{co}}-\frac{T_g}{T_{co}}+E)} \quad (3.26)$$

Where $Xs(q) = X(q)$, $E=a^2q^2/Tco$

For the spin glass condition,

$$g^{SG}(q,\omega) = \frac{1}{2\pi N}\int_{-\infty}^{+\infty} dt e^{-i\omega t}\sum_{ij}\left[\langle S_i(t)S_j(0)\rangle e^{ir.R_{ij}} - \langle S_i\rangle\langle S_j\rangle\right] \quad (3.27)$$

Where[3.27] is the configuration average, Insert eqn (3.27)in to eqn(3.12),we can get.

$$\frac{\tau_{AG}}{\tau} = \frac{1}{2K_F^2\mu^2T_g}\frac{1}{2\pi N}\int^{2K_F} qdq \int_{-\infty}^{+\infty}\frac{\beta\omega}{e^{\hbar\omega}-1}d\omega\int_{-\infty}^{+\infty} dt e^{-i\omega t} * \sum_{ij}\left[\langle S_i(t)S_j(0)\rangle e^{ir.R_{ij}} - \langle S_i\rangle\langle S_j\rangle\right] \quad (3.28)$$

$\{S_i(\infty)S_j(0)\}=Q_{ij}$ and $\{(S_i)\} = 0$ in the time independent.

$$\frac{\tau_{AG}}{\tau} = \frac{Q}{S(S+1)} + \frac{1}{2K_F^2 S(S+1)} \int_{-\infty}^{+\infty} qdq \int_{-\infty}^{+\infty} d\omega \frac{\beta^2\omega^2}{(e^{\beta\omega}-1)^2} K_\beta T X(q) F(q,\omega) \quad (3.29)$$

From eqn (3. 30) $\beta^2\omega^2/(e^{-\beta\omega}-1)^2 = 1$

than,

$$\frac{\tau_{AG}}{\tau} = \frac{Q}{S(S+1)} + \frac{K_\beta T}{2K_F^2 S(S+1)} \int_{-\infty}^{+\infty} qdq \int_{-\infty}^{+\infty} d\omega \, TX(q)F(q,\omega) \quad (3.30)$$

and substitute F(q,ω) from eqn(3.0.24) in to eqn(3.0.34)

$$\frac{\tau_{AG}}{\tau} = \frac{Q}{S(S+1)} + \frac{1}{2K_F^2 S(S+1)} \int_{-\infty}^{+\infty} qdq \int_{-\infty}^{+\infty} d\omega \, K_\beta T \, X(q) \frac{1}{\pi} \frac{Dq^2}{\left(Dq^2\right)^2 + \omega^2}$$

$$= \frac{Q}{S(S+1)} + \frac{1}{2\pi K_F^2 S(S+1)} \int_{-\infty}^{+\infty} X(q) qDdq \int_{-\infty}^{+\infty} d\omega \frac{1}{\left(Dq^2\right)^2 + \omega^2} \quad (3.31)$$

When the spin glass case take D_0 = D a constant, However, the result are not dependent for $F(q,\omega)$ both above and below the transition Tg from equation, and use the above expression.

$$\frac{\tau_{AG}}{\tau} = \frac{Q}{S(S+1)} + \frac{1}{S(S+1)} \frac{1}{2K_F^2} \int_{-\infty}^{+\infty} X(q) qDdq \int_{-\infty}^{+\infty} d\omega \frac{1}{\left(Dq^2\right)^2 + \omega^2}$$

$$= \frac{Q}{S(S+1)} + \frac{K_\beta T}{S(S+1)} \frac{D_0}{2\pi K_F^2} \int^{2K_F} X(q) qdq \int_{-\infty}^{+\infty} d\omega \frac{1}{(Dq^2)^2 + \omega^2}$$

$$= \frac{Q}{S(S+1)} + \frac{K_\beta T}{S(S+1)} \frac{D_0}{2\pi K_F^2} \int^{2K_F} X(q) qdq \left[\frac{1}{\pi} * \pi\right]$$

$$= \frac{Q}{S(S+1)} + \frac{D_0 K_\beta T}{2K_F^2} \int^{2K_F} \left[\frac{X(q)}{(T - T_g + a^2 q^2)}\right] dq \quad (3.32)$$

When use this form for $F(q,\omega)$ both above and below transition temperature T_g at low temperatures, we do not have well define like diffusive type. eqn(3.31) and eqn(3.32) combine together For x (q), we neglects the dependence and can get

$$X(q) = \begin{cases} \frac{S(S+1)}{K_F T_\beta} & T \geq T_g \\ \frac{S(S+1)}{K_\beta T_\beta} & T \leq T_g \end{cases} \quad (3.33)$$

For above T_g we use the usual paramagnetic result, but below T_g We take x to be constant in experimental result. The quality Q is like an order parameter for spin glass,

$$Q = (S^2(1 - T/T_g)) \quad (3.34)$$

Substitute eqn (3.34) in to eqn (3.32), we can get

$$\frac{\tau_{AG}}{\tau} = \frac{S^2(1 - T/T_g)}{S(S+1)} + \frac{D_0 K_\beta T}{2k\beta} \int^{k_F} q \frac{X(q)}{(T - T_g + a^2 q^2)} dq$$

$$= \frac{S^2(1 - T/T_g)}{S(S+1)} + B\left(\frac{T}{T_g}\right) \ln\left(T_{CO}\left(\frac{T}{T_{CO}} - \frac{T_g}{T_{CO}} + E\right)\right)$$

where $B=D_0/4(aK_F)^2$ and $E = (2KFa)^2 T_C$ for X_{AG}/X can get from eqn(3.26) and eqn(3.33)

$$\frac{X_{AG}}{X} = \frac{K_\beta}{4\pi^2 T_{CO}\left(S(S+1)\right)\tau_{AG}\left(\frac{T}{T_{CO}} - \frac{T_g}{T_{CO}} + E\right)} \quad (3.38)$$

$$\frac{X_{AG}}{X} = \frac{A}{\left(\frac{T}{T_{CO}} - \frac{T_g}{T_{CO}} + E\right)} \quad (3.39)$$

Where

$$A = \frac{K_\beta}{4\pi^2 T_{CO}(S(S+1))T_{AG}},$$

Graphical Description

Temprature dependence of the inverse spin – flip scattering time

Figure 12 shows that the ratio of impurity transition temperature T/T_M increases the ratio of AG retardation time T_{AG}/T.

Figure 13 shows that the ratio of temperature with magnetic impurity transition temperature T/T_M increases the ratio of AG retardation time T_{AG}/T also increase.

Phase Diagram of FST Compound

Figure 14 shows that the ratio of temperature with magnetic impurity transition temperature T/T_{CO} increases but as susceptibility X(q) decreases.

Phase Diagram of Spin –Glass in FST Compound

Figure 15 shows that the ratio of temperature with magnetic impurity transition temperature increases but ac susceptibility $X(q)$ increases.

Phase Diagram of FST Compound

Figure 16 shows that the coexistence of temperature with magnetic impurity superconductivity transition temperature T/T_{GO} increases but acsusceptibility $X(q)$ increases.

Conclusion

Superconductivity and magnetism were

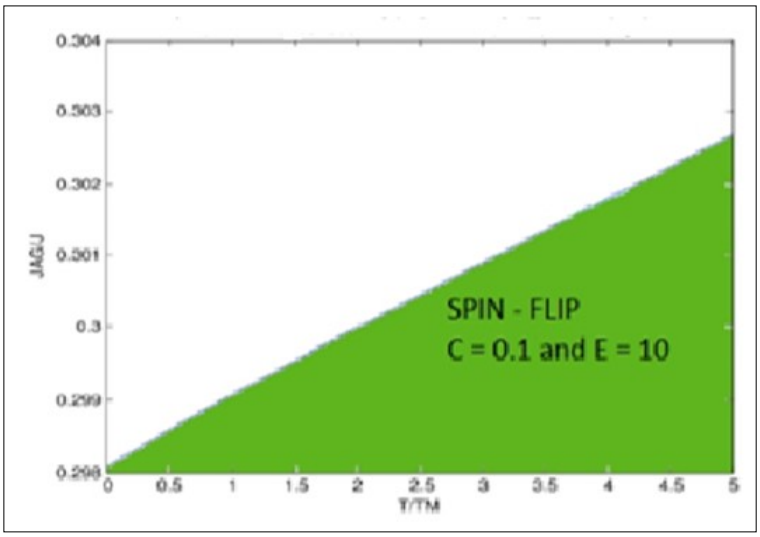

Figure 12. Temperature dependence of the in verse spin-flip Scattering time $1/\tau$ normalized with $1/\tau_{\wedge G}$, where C =0.1 and E = 10 for large T the AG result in Fe1+ySexTe1−x.

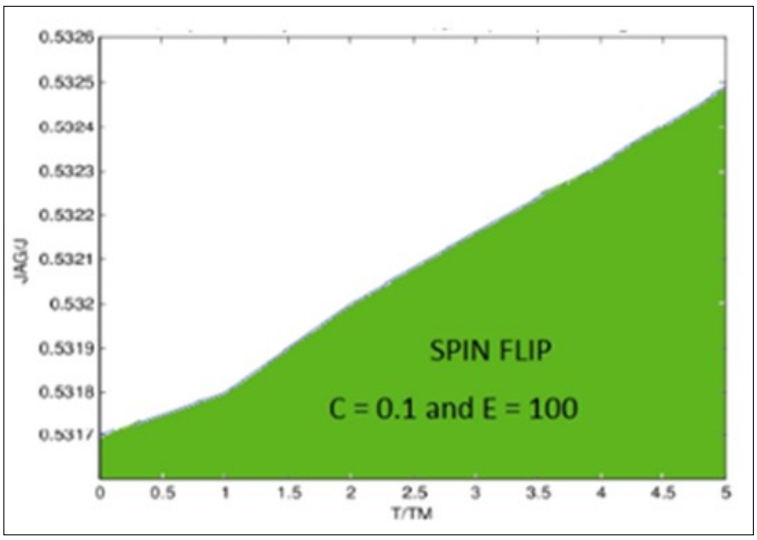

Figure 13. Temperature dependence of the inverse spin-flip Scattering time normalized with ,where C = 0.1, and E = 100 for large T the AG result in $Fe_{1+y}Se_xTe_{1-x}$

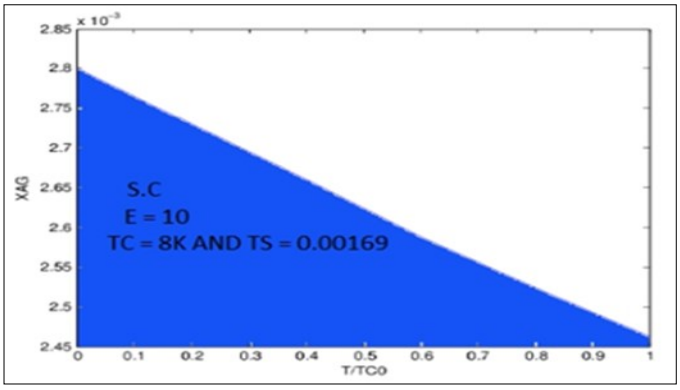

Figure 14. Phase diagram for Fe1+ySexTe1-x its how the superconducting transition temperature for E=10 take Tc=8K and τ_s = 0:00169

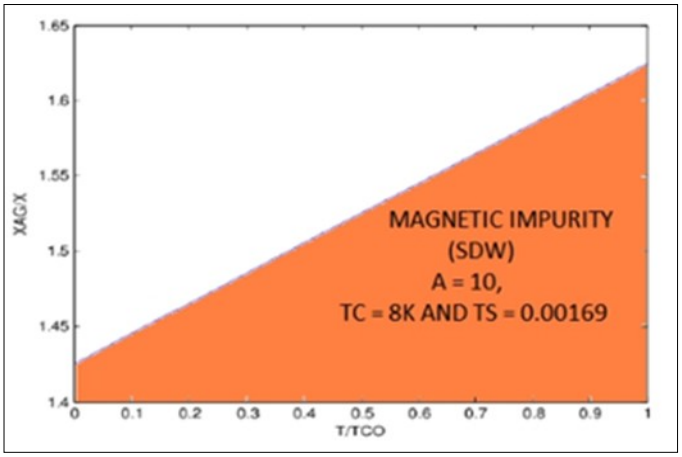

Figure 15. Phase diagram for $Fe_{1+y}Se_xTe_{1-x}$ it show the Superconducting transition temperature for A=5 and E =10 take Tc = 8K and τ_s = 0.00169

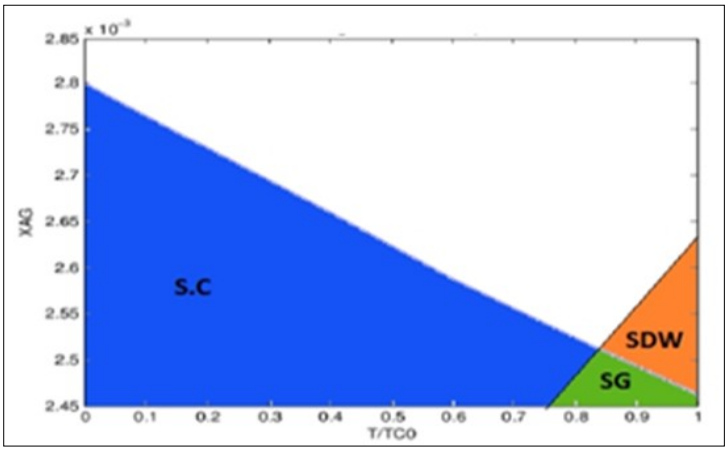

Figure 16. Phase diagram for $Fe_{1+y}Se_xTe_{1-x}$ it show the Superconducting transition temperature for A= 5 and E = 10 take Tc = 8k and τ_s = 0.00169

previously thought as incompatible in BCS theory the superconductor explain in magnetic field which is turn destroy superconductivity. The discovery of some rare earth ternary compounds that shows the superconductivity and magnetic order in system are coexist. The random of magnetic Mostly the superconductivity coexist with spin glass occur in(122) and (11) family, because they have vary at low critical temperature and mobile electrons or holes are doped in to ant ferromagnetic elements like Te or Se parent compound from $Fe_{1+y}Se_xTe_{1+x}$.

The observation of superconductivity with zero resistance critical transition temperature at 8K in the *PbO* type *FeSe* compound known as 11 family.The crystal structure is based on *FeAs* layer of tetragonal shape chemical form type *FeSe* compound known as 11 family.

Acknowledgement

I would like to express my sincere gratitude to my advisor Prof.P.Singh for his Unlimited and constructive guidance, advice, suggestions and comments during my work. I am also thank ful *Dr Mulugeta* to give sum suggestion and comments, I am grateful to all my families.

References

1. Annu.Rev.Condensed.Matterhys.2011.2:16.1-16.20.
2. Dissertationiniron-Pnictide and Cuprate High temperature Superconductors Investigated Photoemission. Spectroscopy by Walid Malaebin june2009.
3. D.K Prettelal, Euro Phys. Rev. Lett103,087001 (2009).
4. WangC,LiL,ChiS,ZhuZ,RenZ,et al.2008.Europhys.Lett.83:67006
5. CBernhardetal.,NewJ.Phys.11,055050(2009).
6. W.Baoetal.,Phys.Rev.Lett.102,247001(2009).[9] S.Lietal.,Phys.Rev.B79,054503(2009).
7. A.Martinellietal.,arXiv:1002.3517v1.
8. Y.Qiuetal.,Phys.Rev.Lett.103067008(2009).
9. S.-H.Leeetal.,arXiv:0912.3205v1.
10. D.N.Argyriouetal.,arXiv:0911.4713v1.[14] Y.Qiuetal.,Phys.Rev.Lett.103067008(20 09)
11. S.LietalarXiv:1001¿1505
12. spin glassan do there Frustrated systems. By Do bashish Chow dhury
13. K.Yamada,2andJ.M.Tranquada:.,
14. arXiv:1003.4525v1[cond-mat2010].
15. Msc Thesis on(FeAs)basedonS.CbyMonilcaBahurup, March2009.
16. Fang,M.H.;Pham,H.M.;Qian,B.;Liu,T.J.;Vehstedt,
17. E.K.;Liu,Y.;Spinu,L.;Mao,Z.Q.Phys.Rev.B2008,78,224 503.
18. Yeh,K.W.;Hsu,H.C.;Huang,T.W.;Wu,P.M.;
19. Huang,Y.L.;Chen,T.K.;Luo,J.Y;
20. Seminar presentation based on Iron base superconducting
21. Knistj an Anderle doc.DavisAR CON(March2011).
22. Msc tessis on the study in coexistence of superconductivity and spin density wave by Dagne Atnafu.JULY2010.
23. K.Yamada, 2 andJ.M.Tranquada:.,arXiv:1003.4525v1 [cond-mat2010].
24. Sarita Khar ka and P.Sing Phys.state.sol. (b),1-10 (2006)/DoI.10.1002/passb200542285.
25. Solid state physics Kittel. Luo,J.Y.; Yan,D.C.; Wu, M.K. Eur. Phys. Lett. 2008, 84, 37002.
26. Fang, M. H.; Pham, H.M.; Qian, B;Liu,T.J.;Vehstedt,
27. Seiminar pressentation based on Iron base superconducting Knistjan Anderle doc. Davis ARCON (March 2011).
28. Yeh,K.W.;Hsu,H.C.;Huang,T.W.;Wu,P.M.;Huang,Y.L. ;Chen,T.K.;Luo,J.Y;
29. Statistical physics of spin glass and information processing (HIDETOOSHI.NISHIMORI)
30. L.Paulose, C.S. Yadav,and K.M. Subhedar. Magnetic phase diagram of *Fe*1+*yTexSe*1*x* system: Coexistence of spin glass behavior with superconductivity? ArXiv: 0907.3513, 2009.
31. Introduction to Disordered Systems and Spin Glasses Gautam I.Menon and Puru sattam Ray.
32. Msc tessis on the study in coexistence of superconductivity and spin density wave by Dagne Atnafu. JULY 2010.